AMSE Association for the Advancement of Modelling & Simulation Techniques in Enterprises
IIETA International Information and Engineering Technology Association
Advancing the World of Information and Engineering

Modelling, Measurement and Control A
Vol. 91, No. 3, September, 2018, pp. 114-122
Journal homepage: http://iieta.org/Journals/MMC/MMC_A

Modelling and analysis of a hybrid controller applied to the ultracapacitor based solar powered electric vehicle

Raghavaiah Katuri*, Srinivasarao Gorantla

Department of Electrical and Electronics Engineering, Vignan's Foundation for Science, Technology, and Research, Vadlamudi, Guntur 522213, Andhra Pradesh, India

Corresponding Author Email: rk_eeep@vignanuniversity.org

https://doi.org/10.18280/mmc_a.910303

Received: 25 July 2018
Accepted: 15 September 2018

Keywords:
solar power, Hybrid Electric Vehicles (HEVs), Bidirectional Converter (BDC), Unidirectional Converter (UDC), battery, ultracapacitor, Math Function Based (MFB) controller, Proportional Integral (PI) controller

ABSTRACT

The high power density capability of Ultracapacitor (UC) can be utilized by developing of Hybrid Energy Storage System (HESS) with a conventional power source, battery. UC power mainly used during peak power requirement of electric vehicle (EV) / Hybrid electric vehicle (HEV) on the other hand side battery is treated as a main source of the entire system and it serves the average power to the load. Energy management between the sources, is the primary difficulty associated with HESS powered electric vehicles. The main aim of this work is to design a new control strategy approach which is used to switch the power sources according to the electric vehicle dynamics. Four math functions are created individually according to the speed of an electric motor, named as Math Function Based (MFB) controller. The designed MFB controller is combined with a Proportional Integral (PI) controller in order to achieve the main objective and applied to the solar-powered electric vehicles for a smooth transition between battery and UC. The principal goal of the designed MFB controller always regulates the pulse signals generated by the conventional PI controller, and this scenario happens with respect to the speed of an electric motor. A solar panel is connected to the electric vehicle which is used to charge the battery charge based on irradiance, temperature available conditions and discharge the same amount of energy during unavailable timings of sunlight All modes of the circuit is simulated in MATLAB and results are plotted, discussed in simulation results and discussion section.

1. INTRODUCTION

Fossil fuel quantity is reducing day to day due to more usage and is not available abundantly in nature. In the conventional scenario, petrol is one of the major fossil fuel for vehicle propulsion. All conventional vehicles are made with IC Engine which demands the petrol/diesel for its proper operation. Several drawbacks are associated with IC engine based vehicle; in that pollution is the main problem and cost of fuel. After several years the conventional fuel will disappears due continuous usage. In order to retain some amount of fossil fuel like crude oil for future generation must have to take a diversion from the use of fossil fuel with other alternative fuel of effective working condition. With all the above reasons using an IC engine is demanding an alternative source for transportation purpose.

Solar power based electric vehicles are designed with battery. Here battery gets charged from solar power during sunlight available times. The designed solar panel is inserted into the vehicle itself to enhance the driving range of an electric vehicle [1]. A solar power station was developed for plug-in electric vehicle charging. If the internal solar power rating power is not sufficient to charge the battery the designed external power station might be useful [2-3]. For small urban electric vehicles, energy management architecture has developed. Different characteristics contained energy sources are integrated like high power density and high energy density. For splitting energy properly between two energy sources rule-based metaheuristic controller is designed by considering different load conditions on the electric vehicle [4]. A new controller strategy approach is designed to switch the energy sources of HESS according to the speed of an electric motor [5-6].

Various characteristics contained multiple sources are combined by the hybridization concept for an electric vehicle application. Here UC and battery are combined and forms HESS with average power can pump by the battery on other hand peak power can be feed by UC. HESS improves the life cycle of battery by demising the number of charging and discharging periods, this can be achieved with UC only. The efficient combination UC and battery forms better energy storage system than the conventional single battery or fuel cell by fulfilling the all road condition of the electric vehicles [7-10].

In order to meet the unexpected driver behavior and different load condition, HESS is designed with various artificial intelligence techniques. Recent preachers mostly concentrating on the optimal usage of fuels which are used to drive the electric vehicles mainly on batteries and different algorithms are proposed to find the optimal way of utilizing the energy sources [11-14].

Novel HESS is developed with low rating DC-DC converter further it can be compared with conventional HESS, which having large power rating DC-DC converter topology. In designed HESS battery end maintains lower voltage value where UC end maintains higher voltage value. Here UC will

supplies the power to the drive until its voltage level is less than the battery voltage level with that comparative constant load is created for the battery [16]. In addition, the battery is not used to directly harvest energy from the regenerative braking; thus, the battery is isolated from frequent charges, which will increase the life of the battery

An improved soft switching method is suggested for the bidirectional converter (BDC) as well as a unidirectional converter (UDC) with coupled inductors. Hysteresis current controller is used for zero voltage switching up to the maximum load range [17]. An effective energy storage system is developed for HEVs/EVs with the neural network controller. The suggested system reduces the energy requirement of the electric vehicle [18].

An effective control strategy is designed to provide the crest power requirement from UC within 20sec. In remaining all cases average power can be supplied by a battery for electric vehicle [19]. A polynomial control is used for better power management between UC and battery. Here battery is connected directly to the dc link whereas UC is connected through BDC to dc link. PIC18F4431 microcontroller is used for a DC-DC converter for proper power-sharing [20]. A new control strategy is designed and implemented, to switch the energy sources present in the HESS according to the electric vehicle dynamics [21].

The main aim of this work is to design a hybrid controller combining Math Function Based (MFB) controller with PI controller for smooth switching between the battery and UC. Additionally PV panel added for changing the battery during sunlight available timings. This work is structured as follows. Section II Presents the proposed system model. Section III includes the PV array mathematical modeling. Section IV describes the Math function based controller. Modes of operation of converter model presented in section V. Section VI presents the proposed model control strategy. Section VII describes simulation results and discussions. Finally, the main conclusions are presented in section VIII.

2. PROPOSED SYSTEM MODEL

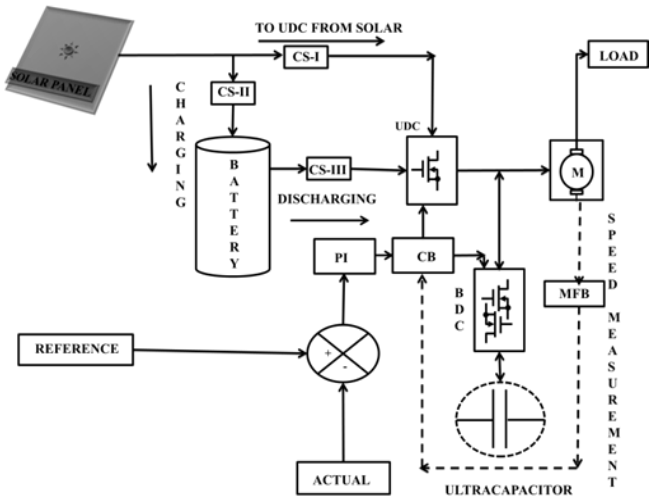

Figure 1. Proposed block diagram model of the hybrid energy Storage system

Figure 1 represents the block diagram model of the HESS including a solar panel for battery charging during sunlight available periods. Here MFB controller output and conventional PI controller outputs are compared at the circuit breaker section and send the required pulse signal to the particular converter according to the electric motor speed. Here PI controller always generates the pulse signal to BDC as well as UDC by comparing reference and the actual voltage level of the converters whereas the MFB controller regulates the pulse signals generated by the PI based on the speed of an electric motor. Additionally, here the solar panel is connected for charging the battery. UC will supply the transient power requirement of the motor whereas battery can supply the average power to the motor.

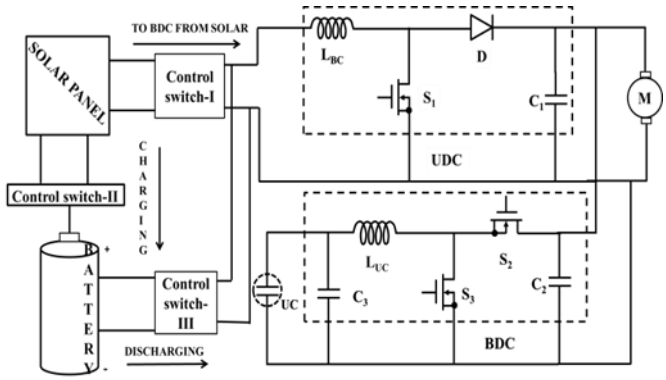

Figure 2. Converter model circuit diagram with HESS

Above figure 2 represents that the converter model circuit diagram of HESS which consisting of the Bidirectional converter (BDC), Unidirectional converter (UDC), battery, Ultracapacitor (UC) and solar panel with three main switches named as S_1, S_2, S_3. The switch S_1 is always in ON condition except for a heavy load condition. Here the solar panel is connected to UDC as well as a battery through control switches I, II and battery are connected to UDC through control switch-III. The charging and discharging timings of the battery are decided by the control switches (CS) action. Here a major part of power can be supplied by the battery only on the other hand auxiliary power can be supplied by UC, that may be starting and transit period of the electric motor.

3. PV ARRAY MATHEMATICAL MODELING

Single PV cell is capable of generates an output voltage of less than 1 V i.e. each Si photovoltaic cell develops the output voltage of around 0.7 V during open circuit time and 0.5 V under working condition. A number of cells are connected in series and parallel to form a PV module and a number of modules are allied in series and parallel to produce the required output. Using Si-based photovoltaic modules the PV system converts only 15% of solar energy into electricity. Ideal solar PV cell is demonstrated by a current source and an inverted diode coupled in parallel to it as shown in Figure 3. The current source represents the current generated by photons denoted as I_{cell} and its output is constant under constant temperature and constant light incident radiation. The practical behaviour of the cell is deviated from ideal due to the optical and electrical losses. There are two key parameters as short-circuit current (I_{sc}) and open circuit voltage that is frequently used to characterize a PV cell. By short-circuiting the terminals of the cell the photon generated current as shown in Figure 3(b), flows out of the cell called as a short circuit current (I_{sc}). Thus, we can say that $I_{cell} = I_{sc}$ as the current

I_{cell} is flowing in a single series circuit. As the terminals are short-circuited then the voltage across the circuit is equal to zero i.e. $V_{oc} = 0$ and the short-circuit current is the PV cell load current (or the output current which is very maximum as equal to that of the current source or photovoltaic photon generated current i.e. $I_{cell} = I_{sc} = I_m$ Similarly, when the terminals are open circuited i.e. no load and nothing is connected as represented in 3 (c), the load current of a PV cell becomes zero. And the load voltage of a PV cell is equal to the maximum applied source voltage or open circuit voltage i.e. $(V_m = V_{oc})$.

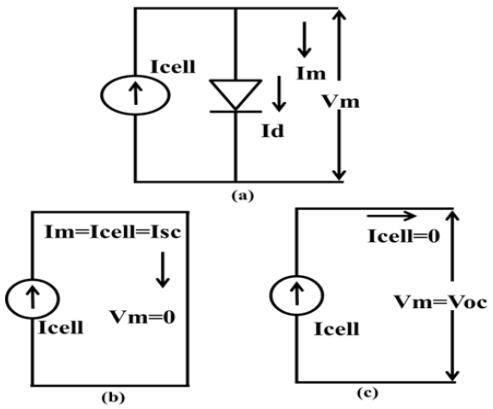

Figure 3. (a) PV cell equivalent circuit, (b) PV cell at short circuit condition (c) PV cell at open circuit condition

The PV cell output current can found by applying KVL to circuit 1(a),

$$I_m = I_{cell} - I_d \quad (1)$$

The current through diode can be represented with bellow equation

$$I_d = I_{rscell}\left[e^{\left(\frac{QV}{KT_{ap}}\right)-1}\right] \quad (2)$$

By replacing Id in Equation 2, it gives the current-voltage relationship of the PV cell as shown below

$$I_m = I_{cell} - I_{rscell}\left[e^{\left(\frac{QV}{KT_{ap}}\right)-1}\right] \quad (3)$$

The diode reverse saturation current (I_{rscell}) is constant under the constant temperature and irradiance that is calculated by the open circuit condition of PV cell as illustrated in Figure 3(b). From the Equation (3) it is observed that $I_m = 0$ and solve for I_{rscell}

$$I_{rscell} = \frac{I_{cell}}{\left[e^{\left(\frac{QV}{KT_{ap}}\right)-1}\right]} \quad (4)$$

The photon generated current is directly proportional to the irradiance and temperature, whereas the voltage is directly proportional to the irradiance and inversely proportional to the temperature. The value of I_{scr} is provided by the manufacturer datasheet at STC (standard test condition). At STC, the working temperature and irradiance are 25^0 C and 1000 W/m respectively.

In the present work, the standard PV array is taken and generated the power with different temperature, irradiance values. Thereafter using DC-DC converter solar panel voltage changed according to the electric vehicle requirement. Here tree control switches are connected to the solar panel, battery, and UDC. State of charge of the battery and the output voltage of the solar panel decides the control switches action.

4. MATH FUNCTION BASED CONTROLLER (MFB)

The designed hybrid controller is a combination of MFB controller and PI controller, in that PI controller generates the pulse signals whereas the MFB controller regulates the pulse signals according to the speed of an electric motor. The MFB controller generates the controls signal in four modes as follows.

(1) If the speed of the motor is less than or equal to 4800 rpm then MFB generates signal U_1 as 1.

(2) If the speed is in between 4600 rpm to 4800 rpm then MFB generates signals U_1 and U_2 as 1.

(3) If the speed of the motor lies between 4801rpm to 4930rpm MFB generates signal U_3 as 1.

(4) If the speed of the motor is greater than or equal to 4931 rpm MFB generates signal U_4 as 1.

All the above signals are used to perform the smooth switching between the battery and UC which means switching between sources can be done by MFB controller combined with the PI controller. Here U_1, U_2, U_3, and U_4 are the output signals of the designed MFB controller.

5. MODES OF OPERATION OF CONVERTER MODEL

The proposed work can be analyzed in four modes with different loads. All four mode condition with different loads and switches ON and OFF condition illustrated in below table 1.

5.1 Mode-I operation

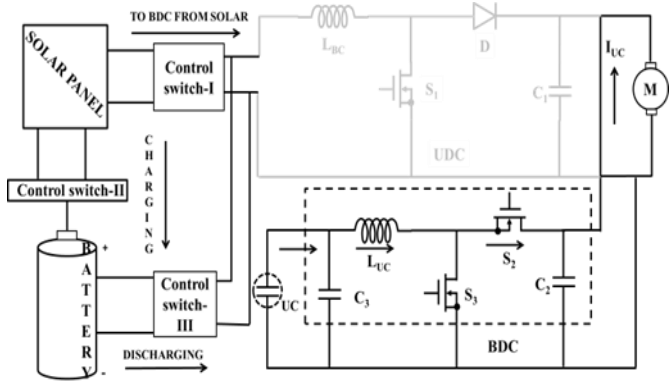

Figure 4. Converter Mode-I circuit diagram with HESS

Table 1. Load condition based switching action

Mode	S1	S2	S3	Load Torque
I	OFF	OFF	ON	Heavy Load
II	ON	OFF	ON	Medium Load
III	ON	OFF	OFF	Rated load
IV	ON	ON	OFF	No Load

During Mode-I operation a heavy load is applied to the electric motor. Generally, at starting and transient period of vehicle UC can supply excess power which is a burden on the main source, battery. In this configuration, the battery is charging from the solar panel during irradiance and temperature available periods and discharges the same amount of energy during the odd time (unavailability of sunlight). In this mode switch, S_3 is only in ON position remain two switches S_1 and S_2 are in OFF position. Total power flows from UC to the electric motor and no power flows from the battery side.

5.2 Mode-II operation

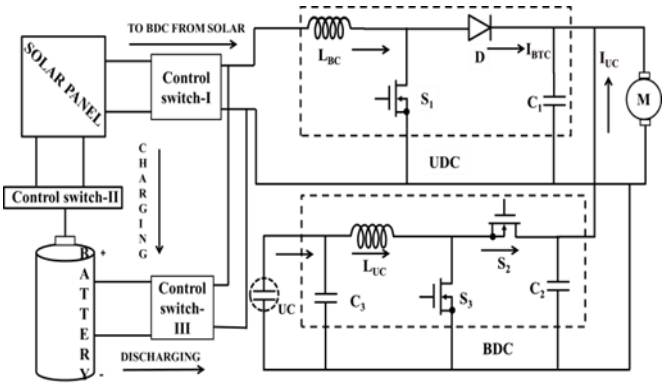

Figure 5. Converter Mode-II circuit diagram with HESS

Mode-II is related to slightly more than the rated load on the electric motor. During this condition switches S_1, S_3 are in ON condition and switch S_2 is in OFF position. During this mode of operation battery and UC together supplies required power to the electric motor. Depending upon the control switches actions which are connected at the battery, solar panel, and UDC, solar energy is directly connected to UDC or battery is connected directly to UDC. Entire power will flow from battery plus UC to load.

5.3 Mode-III operation

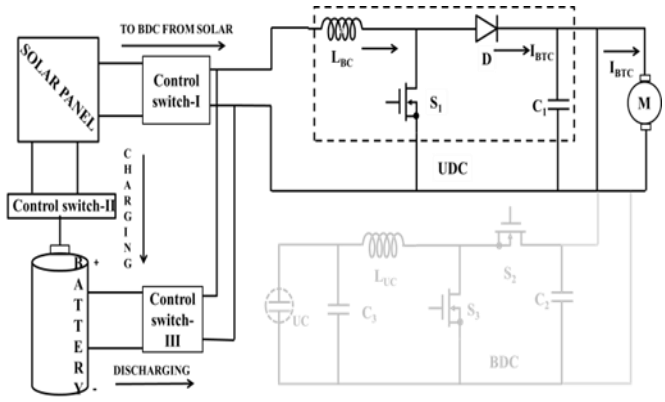

Figure 6. Converter Mode-III circuit diagram with HESS

In this mode of operation, a rated load is applied to the electric motor. So switches S2, S3 are in OFF position and remain switch S1 is in ON position. During rated load condition entire power can be supplied by the battery itself and no power can be supplied by UC. During this mode of operation, total power flows from battery to the load and no action is required by the UC. Depending upon the battery SOC and terminal voltage of solar panel the control switches will respond, based on that power can flows directly to UDC or from the battery.

5.4 Mode-IV operation

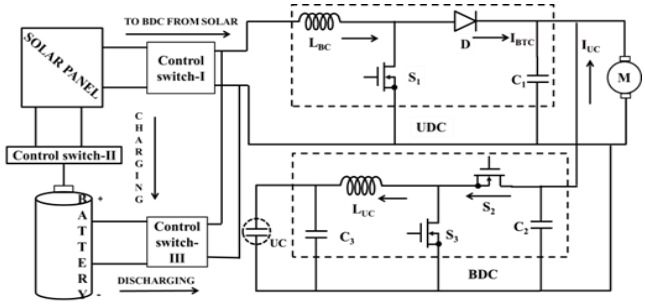

Figure 7. Converter Mode-IV circuit diagram with HESS

No load applied to the electric motor is related to Mode-IV operation. In this mode, the battery is able to supply power to the electric motor as well as for UC charging. So the switches S_1, S_2 are in ON condition and S_3 is in OFF position, which means, UDC working as boost and BDC working as buck converter for UC charging. The connected solar panel is used here to charge the battery during sunlight available periods.

6. PROPOSED MODEL CONTROL STRATEGY

The designed hybrid controller controllers the pulse signals of two converters depending upon the speed of the electric motor. It can be categorized into four modes of operation. During mode-I operation pulse signals are generated to only switch S_3 ,in mode-II operation pulse signals generate to switch S_1 as well as switch S_3, in mode-III pulse signals generates only to S_1 and during mode-IV operation pulse signals generated to switch S_1 as well as switch S_2.

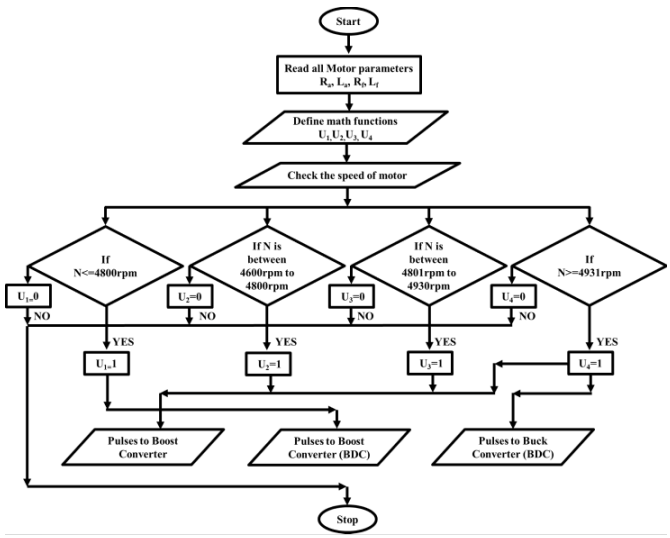

Figure 8. Flowchart of the control strategy

(1) While starting of a motor and heavy loaded condition UC supplies require power to the load. In this mode, the math function U_1 gives signal value as 1 and remaining all math functions generates a signal as 0 because during this period the

speed of the motor is ≤ 4800 rpm. The converter operates based on all math function generated signals. The converters in operation are the boost converter at the UC end.

(2) When the power demanded by the load is beyond the designed range of the battery output power, UC will assist the battery to deliver power to the motor. In this mode of operation, motor speed is from 4600 rpm to 4800 rpm. Hence MFB generates U_1 and U_2 pulse signals as 1 and generates U_3 and U_4 pulse signals as 0. The converters in operation are the boost converter at the battery end and the boost converter at the UC end.

(3) When battery output power matches the desired power of the motor, the battery individually supplies the power to the motor. In this mode of operation, the speed of the motor is from 4801 rpm to 4930 rpm. Hence MFB generates a U_3 pulse signal as 1 and generates U_1, U_2 and U_4 pulse signals as 0. During this time, the UDC at the battery terminal works.

(4) When battery provides more power than the motor need, the extra power will be used to charge the UC. So the power of the battery will flow into both the UC and the motor. In this mode of operation, motor speed is >4931 rpm .Hence MFB generates a U_4 pulse signal as 1 and generates U_1 ,U_2 and U_3 pulse signals as 0. According to the converters designed, the

UDC at the battery end and the buck converter (BDC) at the UC end will work in this scenario.

7. SIMULATION RESULTS AND DISCUSSIONS

7.1 Mode-I results

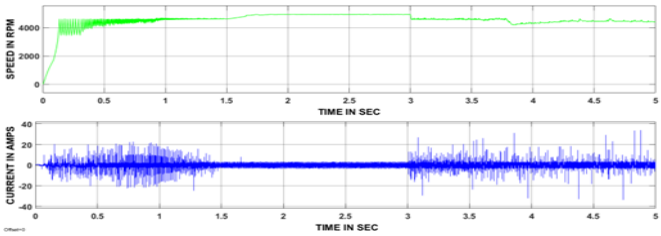

Figure 9. The speed and current responses of the electric motor during a heavy load condition

During starting, 1.8 sec time has taken by the electric motor to reach the steady state. Thereafter at 3 sec, a heavy load is applied to the motor due to that huge current and speed variation will appear which is clear from figure 9. The electric motor speed response doesn't reach the steady state within a stipulated time period due to heavy load.

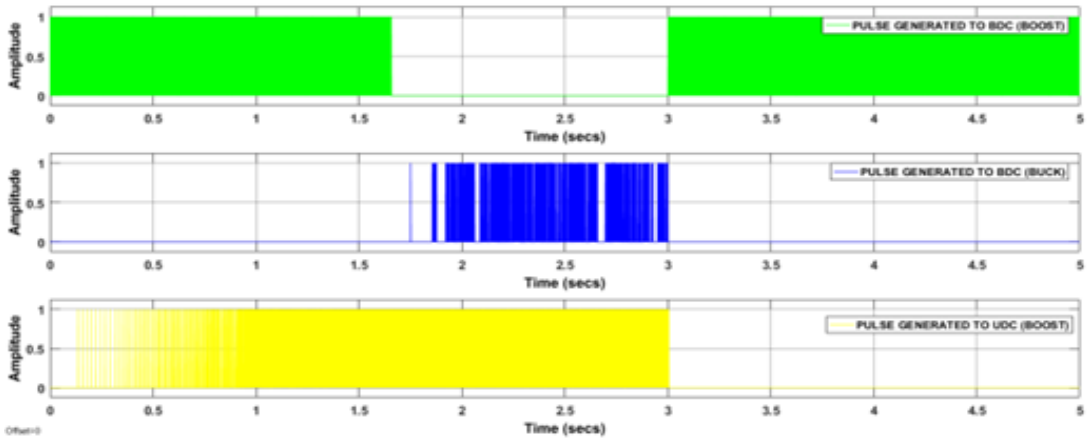

Figure 10. The pulse signals generated by the MFB with PI controller during a heavy load condition

Figure 10 is related to pulse signals generated to BDC as well UDC by the designed controller based on the speed of an electric motor. This mode is related to a heavy load on the motor. During starting of an electric motor total power can be supplied by the UC only after some time UC assist the battery until motor speed response reaching steady state. Thereafter battery only supply energy to the electric motor as well as UC until load applied to the motor, those variations can clearly observe from the figure 10. At 3 sec a heavy load is applied to the motor, during this period pulse signals are generated to BDC working as a boost converter. Which means, during a heavy load condition total power required by the electric motor can supply by the UC only according to the designed controller action.

7.2 Mode-II results

In this mode of operation, slightly more than rated load is applied to the electric motor. After reaching steady state no change can be observed in speed and current responses until a load applied which is clear from figure 11. Thereafter at 3 sec slightly more than rated load is applied to the electric motor, which causes the disturbances in both responses (speed and current) and both reached steady state within 0.2 sec, by the designed controller action.

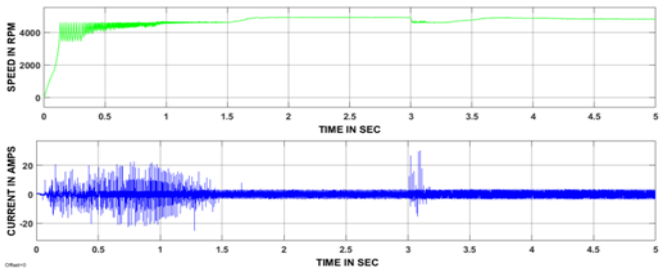

Figure 11. The speed and current responses of the electric motor during slightly more than rated load condition

Figure 12 is related to pulse signals generated to BDC as well UDC by the designed controller based on the speed of the electric motor. This mode is related to slightly more than the

rated load on the motor. During starting of electric motor total power can be supplied by the UC only after some time UC assist the battery until motor speed response reaching steady state. Thereafter battery only supply energy to the electric motor as well as UC until load applied to the motor, those variations can clearly observe from figure 12. At 3 sec slightly more than rated load is applied to the motor, during this period pulse signals are generated to BDC working as a boost converter as well as UDC working as a boost converter. Which means, during slightly more than rated load condition total power required by the electric motor can supply by the battery and UC according to the designed controller action.

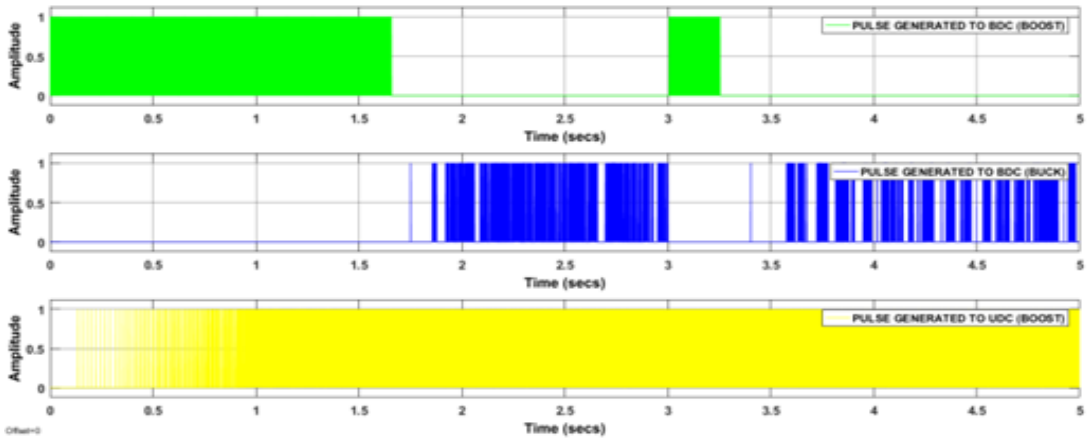

Figure 12. The pulse signals generated by the MFB with PI controller during slightly more than rated load condition

7.3 Mode-III results

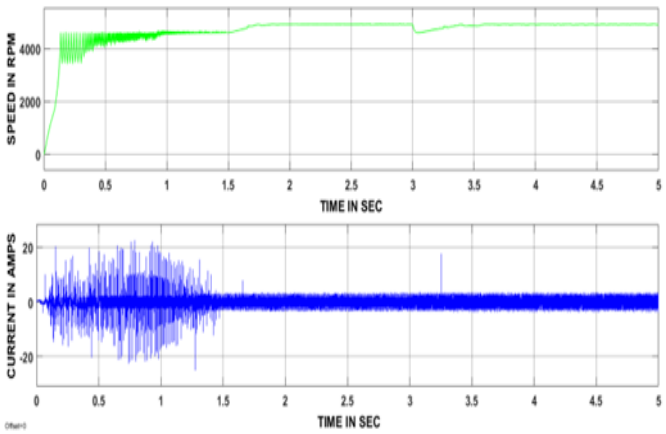

Figure 13. The speed and current responses of the electric motor during a rated load condition

In this mode of operation, a rated load is applied to the electric motor. After reaching steady state no change can be observed in speed and current responses until a load applied which is clear from figure 13. Thereafter at 3 sec, a rated load is applied, which causes the small disturbances in both responses (speed and current) and both responses reached steady state within 0.1 sec, by the designed controller action.

Figure 14 is related to pulse signals generated to BDC as well UDC by the designed controller based on the speed of an electric motor. This mode is related to a rated load on the motor. During starting of electric motor total power can be supplied by the UC only after some time UC assist the battery until motor speed response reaching steady state. Thereafter battery only supplies power to the electric motor as well as UC until load applied to the motor, those variations can clearly observe from figure 14. At 3 sec rated load is applied to the motor, during this period pulse signals are generated to UDC working as a boost converter. Which means during a rated load condition total power required by the electric motor can supply by the battery only according to the designed controller action.

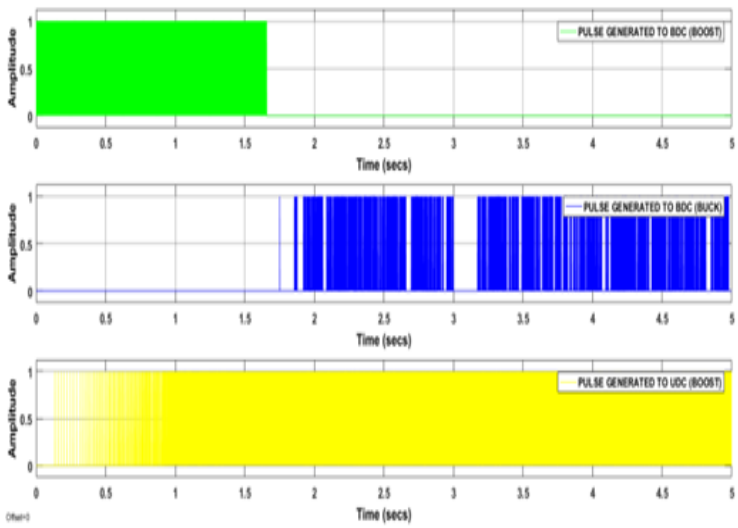

Figure 14. The pulse signals generated by the MFB with PI controller during a rated load condition

7.4 ode-IV results

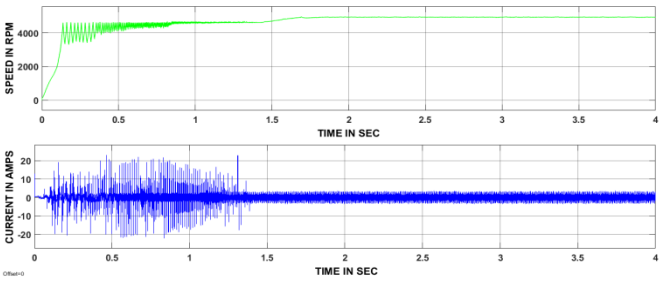

Figure 15. The speed and current responses of the electric motor during no load condition

During this mode of operation, no load is applied to the electric motor. So no disturbances are observed in speed as well as current responses after reaching steady state. During starting, the motor has taken 1.8 sec time to reach the steady state.

Figure 16 is related to pulse signals generated to BDC as well UDC by the designed controller based on the speed of an electric motor. This mode is related to no load on the motor. During starting of electric motor total power can be supplied by the UC only after some time UC assist the battery until motor speed response reaching steady state. Thereafter battery only supplies power to the electric motor as well as UC until load applied to the motor, those variations can clearly observe from the figure 16.

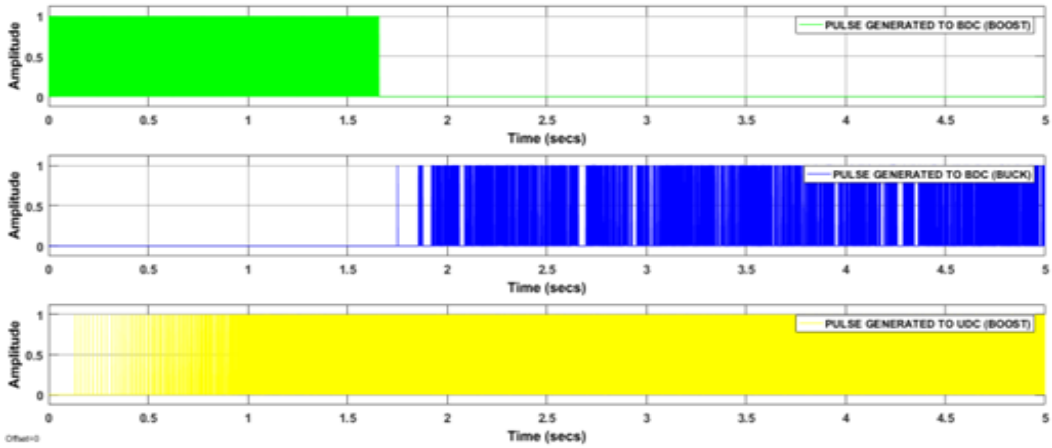

Figure 16. The pulse signals generated by the MFB with PI controller during no load condition

7.5 Battery parameters

In the present work battery minimum SOC has taken 20%, if battery SOC is bellowed 20% then it should get charged from the solar power directly after that again discharges the same amount of power to the electric vehicle until its SOC reaches to 20%. From the above figure 17, it is clear that during discharging time the battery current showing positive whereas shown negative value under the charging period.

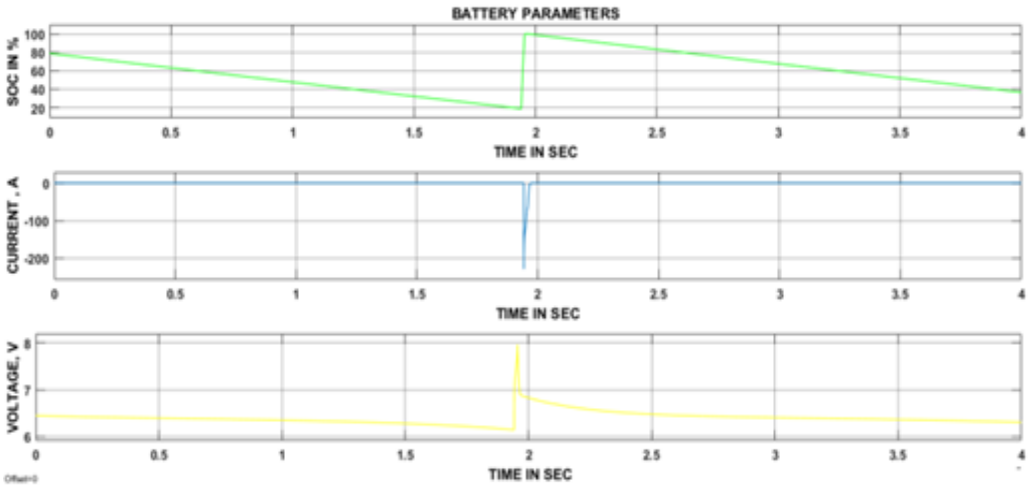

Figure 17. The battery parameters during charging and discharging periods

7.6 Solar panel parameters

Figure 18 represents the solar panel input parameters and duty cycle value connected at the solar panel side. Here solar power can be generated based on the irradiance and temperature availability, because that those two parameters are changed continuously, corresponding to that duty cycle of the converter also changed according to the maximum power point tracking controller action. Different variations of temperature and irradiance can be observed from the above figure 18.

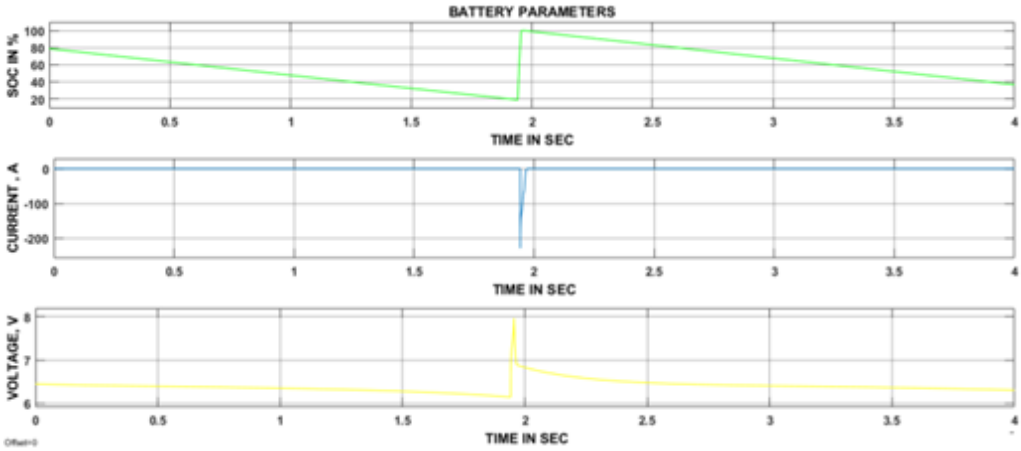

Figure 18. Solar panel parameters and duty cycle of the converter

Table 2. Operation of the converter based on four modes

Mode Condition	UDC	BDC	Mode of Operation
Mode-1	Off	Boost	Power flow UC to Motor
Mode-2	Boost	Boost	Power flow UC+Battery to Motor
Mode-3	Boost	Off	Power flow Battery to Motor
Mode-4	Boost	Buck	Power Flow to Motor and UC From Battery

Table 3. State of math function based on the speed of the motor

Condition Based on Speed of the Motor	State of Math Function
If Speed is ≤4800 rpm	Math function U_1=1
If Speed is from 4600 rpm To 4800 rpm	Math function U_1=1& U_2=1
If Speed is from 4801 rpm To 4930 rpm	Math function U_3=1
If Speed is >4931 rpm	Math function U_4=1

8. CONCLUSIONS

In this paper, a control strategy approach is designed by combining the designed MFB controller with a conventional PI controller and implemented to the solar-powered electric vehicle for a smooth transition between battery and UC. The solar panel is utilized for charging the battery and also directly connected to the electric vehicle through the DC-DC converter. The switching action taking place in HESS based on the speed of the electric motor. The speed is measured by the MFB controllers which initiated the generation of pulses (U1, U2, U3, and U4) thereafter which are compared with PI controller generated pulse signals by means of the circuit breaker in order to obtain the controlled pulse signals to the converters. Which means the designed MFB controller regulated the pulse signal generated by the PI controller based on the speed of an electric vehicle. Finally, the MFB controller combined with a PI controller and generated the controlled pulse signals to the converters BDC as well as UDC based on the electric vehicle requirement. Totally, four modes are simulated for the successful operation of the electric vehicle and obtained the satisfactory results during switching of energy sources with designed MFB controller with PI controller. All modes results discussed and plotted in simulation and discussion section.

REFERENCES

[1] Khan S, Ahmad A, Ahmad F, Shafaati Shemami M, Saad Alam M, Khateeb S. (2018). A comprehensive review on solar-powered electric vehicle charging system. Smart Science 6(1): 54-79. http://dx.doi.org/10.1080/23080477.2017.1419054

[2] Sadagopan S, Banerji S, Vedula P, Shabin M, Bharatiraja C. (2014). A solar power system for electric vehicles with maximum power point tracking for novel energy sharing. In India Educators' Conference (TIIEC), 2014 Texas Instruments, pp. 124-130. IEEE. http://dx.doi.org/10.1109/TIIEC.2014.029

[3] Bhavnani SH. (1994). Design and construction of a solar-electric vehicle. Journal of Solar Energy Engineering 116(1): 28-34. http://dx.doi.org/10.1115/1.2930061

[4] Golchoubian P, Azad NL. (2017). Real-time nonlinear model predictive control of a battery–supercapacitor hybrid energy storage system in electric vehicles. IEEE Transactions on Vehicular Technology 66(11): 9678-88. http://dx.doi.org/10.1109/TVT.2017.2725307

[5] Katuri R, Gorantla SR. (2018). Math function based controller applied to the electric/hybrid electric vehicle. Modeling, Measurement and Control A 91(1): 15-21.

[6] Katuri R, Rao G. (2018). Design of math function based controller for smooth switching of hybrid energy storage system. Majlesi Journal of Electrical Engineering 12(2): 47-54.

[7] Shen J, Khaligh A. (2015). A supervisory energy management control strategy in a battery/ultracapacitor hybrid energy storage system. IEEE Transactions on Transportation Electrification 1(3): 223-31. http://dx.doi.org/10.1109/TTE.2015.2464690

[8] Wu D, Todd R, Forsyth AJ. (2015). Adaptive rate-limit control for energy storage systems. IEEE Transactions on Industrial Electronics. 62(7): 4231-40. http://dx.doi.org/10.1109/TIE.2014.2385043

[9] Emadi A, Lee YJ, Rajashekara K. (2008). Power electronics and motor drives in electric, hybrid electric, and plug-in hybrid electric vehicles. IEEE Transactions on Industrial Electronics 55(6): 2237-2245. http://dx.doi.org/10.1109/TIE.2008.922768

[10] Chan CC, Bouscayrol A, Chen K. (2010). Electric, hybrid, and fuel-cell vehicles: Architectures and modelling. IEEE Transactions on Vehicular Technology 59(2): 589-598. http://dx.doi.org/10.1109/TVT.2009.2033605

[11] Xiang C, Wang Y, Hu S, Wang W. (2014). A new topology and control strategy for a hybrid battery-ultra-capacitor energy storage system. Energies 7(5): 2874-96. http://dx.doi.org/3390/en7052874

[12] Gholizadeh M, Salmasi FR. (2014). Estimation of state of charge, unknown nonlinearities, and state of health of a lithium-ion battery based on a comprehensive unobservable model. IEEE Transactions on Industrial Electronics 61(3): 1335-1344. http://dx.doi.org/10.1109/TIE.2013.2259779

[13] Sánchez Ramos L, Blanco Viejo CJ, Álvarez Antón JC, García García VG, González Vega M, Viera Pérez JC. (2015). A variable effective capacity model for LiFePO4 traction batteries using computational intelligence techniques. IEEE Transactions on Industrial Electronics 62(1): http://dx.doi.org/10.1109/TIE.2014.2327552

[14] de Castro R, Araujo RE, Trovao JPF, Pereirinha PG, Melo P, Freitas D. (2012). Robust DC-link control in EVs with multiple energy storage systems. IEEE Transactions on Vehicular Technology 61(8): 3553-3565. http://dx.doi.org/10.1109/TVT.2012.2208772

[15] Carter R, Cruden A, Hall PJ. (2012). Optimizing for efficiency or battery life in a battery/supercapacitor electric vehicle. IEEE Transactions on Vehicular Technology 61(4): 1526-33. http://dx.doi.org/10.1109/TVT.2012.2188551

[16] Ferreira AA, Pomilio JA, Spiazzi G, de Araujo Silva L. (2008). Energy management fuzzy logic supervisory for electric vehicle power supplies system. IEEE Transactions on Power Electronics 23(1). http://dx.doi.org/107-115. 10.1109/TPEL.2007.911799

[17] Choi ME, Kim SW, Seo SW. (2012). Energy management optimization in a battery/supercapacitor hybrid energy storage system. IEEE Transactions on Smart Grid 3(1): 463-72. http://dx.doi.org/10.1109/TSG.2011.2164816

[18] Trovao JPF, Santos VD, Antunes CH, Pereirinha PG, Jorge HM. (2015). A real-time energy management architecture for multisource electric vehicles. IEEE Trans. Industrial Electronicsb 62(5): 3223-3233. http://dx.doi.org/10.1109/TIE.2014.2376883

[19] Cao J, Emadi A. (2012). A new battery/ultracapacitor hybrid energy storage system for electric, hybrid, and plug-in hybrid electric vehicles. IEEE Transactions on Power Electronics 27(1): 122-132. http://dx.doi.org/10.1109/TPEL.2011.2151206

[20] Zhang Y, Sen PC. (2003). A new soft-switching technique for buck, boost, and buck-boost converters. IEEE Transactions on Industry Applications 39(6): 1775-1782. http://dx.doi.org/10.1109/TIA.2003.818964

[21] Katuri R, Gorantla S. (2018). Simulation and modelling of Math Function Based controller implemented with fuzzy and artificial neural network for a smooth transition between battery and ultracapacitor. Advances in Modelling and Analysis C 73(2): 45-52.